INVESTIGATION OF DIAGNOSTIC TECHNIQUES ON A NONNEUTRAL PLASMA*

K. Schulte[†], M. Droba, O. Meusel, and U. Ratzinger
Institute for Applied Physics, Goethe-University, Frankfurt a. M., Germany

Abstract

Space charge lenses use a confined electron cloud for the focusing of ion beams. The focusing strength is given by the electron density whereas the density distribution influences the mapping quality of the space charge lens and is related to the confinement. The plasma parameters, loss- and production mechanisms have a strong impact on plasma-beam-interactions.

A scaled up space charge lens was constructed to investigate the properties of a nonneutral plasmas in detail.

New non-interceptive diagnostic has been developed to characterize the collective behaviour of the confined nonneutral plasma in terms of an optimized lens design and parameters.

Experimental results will be presented in comparison with numerical simulations.

SPACE CHARGE LENS

The confinement of the nonneutral plasma within the space charge lens is realized by crossed magnetic and electric fields. An electrode system consisting of anode and ground electrode provides a potential well in longitudinal direction while the field of the magnetic coils contains the electrons in radial direction (Fig. 1). If the confined elec-
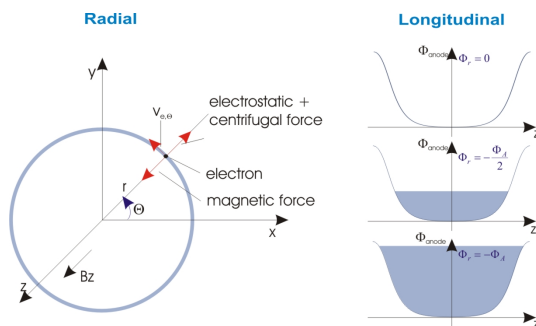

Figure 1: Scheme of the longitudinal and radial confinement principle.

trons are homogeneously distributed, the electron cloud produces a linear electric field in radial direction. As a result of this electric field the application of the space charge lens as a focusing optic for heavy ion beams is advantageous. Besides the independency of focusing from the ion mass, the trapped electrons compensate the space charge force of the beam [1].

However, the theoretical predictions about the nonneutral plasma cloud neglect the interaction of electrons with other particles e.g. residual gas atoms and ions.

To further investigate the properties of the nonneutral plasma as well as the plasma state due to the interaction processes, a scaled-up space charge lens was constructed.

The length of the prototype is 436 mm with an aperture of 150 mm (Fig. 2). The maximum anode potential is Φ_A=50 kV while the maximum magnetic field is B_z=160 mT.
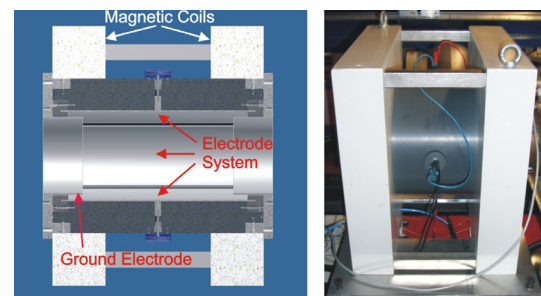

Figure 2: Mechanical drawing (left) and photograph (right) of the space charge lens prototype.

EXPERIMENTS AND DIAGNOSTICS

For the determination of plasma parameters and the associated investigation of diagnostic techniques on a nonneutral plasma various experimental setups have been established.

In the following experiments and diagnostic techniques are described.

Investigation of Residual Gas Ions and Electron Density Measurement

The plasma production begins with an electron originating from natural radioactivity or cosmic rays which acquires its energy from the enclosing fields. Because of the crossed magnetic and electric fields electrons perform a ExB drift while they oscillate within the potential well.

Due to the interaction with the residual gas atoms a avalanche electron production begins. The trapped electrons reduce the on-axis potential while the produced residual gas ions are longitudinally accelerated out of the lens. By measuring the energy of the emitted residual gas ions one can determine the average electron density by:

$$\bar{n}_e = \frac{4\epsilon_0 \Delta\Phi}{er^2} \tag{1}$$

where $\Delta\Phi$ is the difference of the anode voltage and the voltage drop of ions, and r is the radius of the electrode. Measurements show that there are different regions of ion
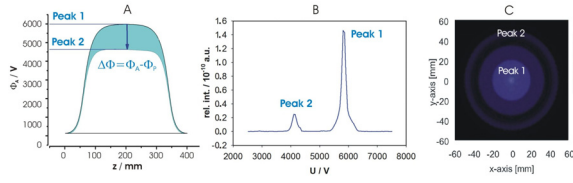

Figure 3: Scheme of electron density measurement technique. (A) represents the potential depression by the electrons and (B) shows the measured ion current for the different production regions within the plasma (C).

production within the electron plasma. This is also validated by numerical simulations (Fig. 3). For determination of the average electron density the inner region (peak 1) plays an important role [2]. Peak 2 results from the ion production in a small zone near the anode.

The measured average electron densities are in good agreement with numerical values.

The detection of the emitted residual gas ions by a pepperpot emittance meter is also used to determine the phase space distribution that yields information about the plasma state (Fig. 4) [3].
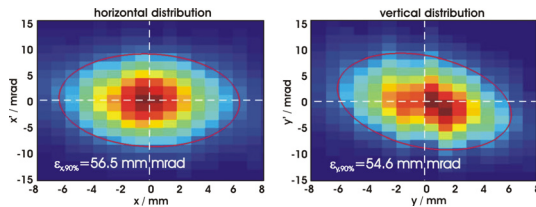

Figure 4: An example of measured transversal phase space distribution of emitted particles from the space charge lens.

Electron Temperature Measurement

The knowledge of the electron temperature is of great importance for the evaluation of the plasma dynamics with respect to loss- and production mechanisms.

Conventional diagnostic methods for determining the electron temperature are not suited for the nonneutral plasma [2]. This is due to the absence of important recombination processes like three body recombination, radiative recombination and the low average electron densities of $n_e = 1 \cdot 10^{14}\,\mathrm{m}^{-3}$.

The application of the corona model requires the knowledge of the collisional-radiative ionization coefficients and still represents a simplified model of the dynamics of the plasma [4]. To overcome the difficulties of electron temperature measurement the determination of T_e by considering the optical-emission cross sections is currently under investigation.

The optical method relates the emitted line intensities to the

cross section for production of excited states by the collision of an electron beam with residual gas like helium [5]. The direct cross section Q_j^d can be expressed by the optical-emission cross sections Q_{ji} and Q_{ki} as:

$$Q_j^d = \sum_i Q_{ji} - \sum_k Q_{ki}, \qquad (2)$$

$$Q_{ji} = \frac{I_{ji}e}{In_0t\Delta x}, \qquad (3)$$

where I_{ji} is the number of emitted photons, I the electron beam current, n_0 the target gas density, and Δx is the length of the electron beam region from which radiation is collected.

Therefore, the electron temperature can be determined by comparing the ratio of two measured optical-emission cross sections to the excitation energy of the electron beam.

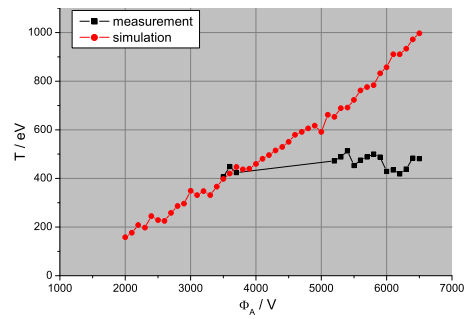Based on this principle the electron temperature using

Figure 5: Measured electron temperature compared to the numerical simulation, $B_z = 8.7$ mT, $p = 4.8 \cdot 10^{-4}$ hPa.

optical-emission cross section data from [6] was determined. Figure 5 shows a clear discrepancy of the results in electron temperature between experimental data and numerical prediction.

To further investigate the relations of excitation processes and to expand the data base of optical-emission cross sections depending on the electron beam energy an addtional experiment has been prepared. First results show a depen-
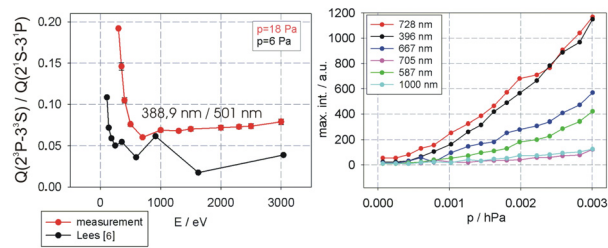

Figure 6: Measured ratio of the optical cross sections as a function of the electron energy and comparison to [6] (left), an example of pressure dependency of emitted line intensities (right).

dency of the detected photon flux on the residual gas pressure. As a consequence this pressure dependency affects

the optical-emission cross sections and might be one reason for the different results shown in Fig. 6.

To evaluate the temperature measurement method, the optical cross sections with respect to the pressure have to be determined.

Nonneutral Plasma Dynamics

Following theoretical predictions similar strengths in longitudinal and radial confinement lead to a homogeneous distribution of electrons in the lens volume and equality of average kinetic energies in both directions. This is represented by the work function of the space charge lens:

$$\Phi_A = \frac{er^2 B_z^2}{8m_e} \tag{4}$$

where Φ_A is the anode voltage, r the radius of the electrode, and B_z the magnetic field.

Far from this configuration a variety of instabilities can be observed. Figure 7C shows the so called diocotron instabil-

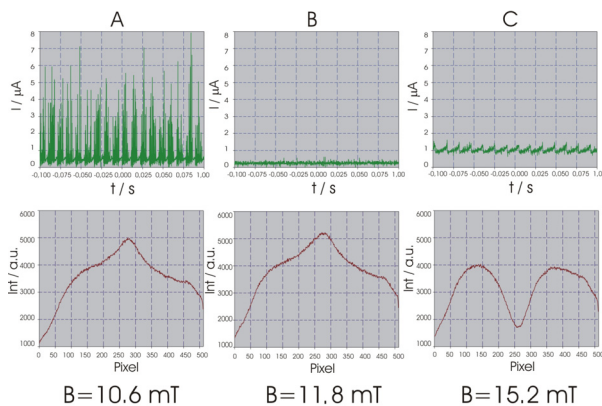B=10.6 mT   B=11.8 mT   B=15.2 mT

Figure 7: Variation of measured residual gas ion current and light density profile in the region of instabilities (A,C) and in the region of the lens' work function (B), Φ_A=4 kV, p=6·10^{-4} hPa, He.

ity. This instability occurs in unneutralized charge sheets of finite width in the presence of a magnetic field and is a result of an interaction between two waves propagating along the sheet surface [7].

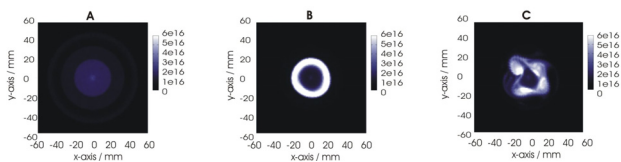A 3D-Particle-In-Cell simulation was used for a better

Figure 8: Numerical simulation of a typical time dependent evolution of a diocotron instabilty in the space charge lens. Picture (A) until (C) represents the density distribution within ns-time steps.

understanding of the time dependent evolution of a diocotron instabilty in the space charge lens due to different

field strengths (Fig. 8) [8].
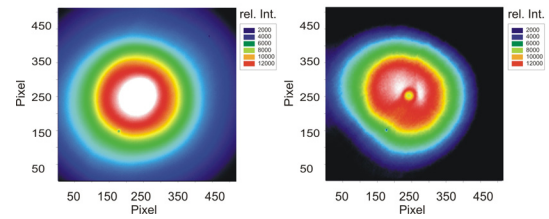
Besides the appearance of the instabilities due to the en-

Figure 9: Picture of a diocotron instabilty for different pressures of helium and similar field strengths, Φ_A=6.5 kV, B_z=12.1 mT, p=7.8·10^{-5} hPa (left) and Φ_A=6.0 kV, B_z=12.1 mT, p=6.0·10^{-4} hPa (right).

closing fields, measurements also show a strong dependency of the plasma state on the residual gas pressure (Fig. 9).

To further investigate the behaviour of instabilities as a function of external parameters the development of a fast optical diagnostic is in progress. Additionally, the pepperpot emittance scanner gives the opportunity of a time-resolved investigation of the plasma state.

CONCLUSION AND OUTLOOK

Methods to determine the plasma parameters have been presented. Non-interceptive diagnostics for the measurement of the electron temperature in a non-equilibrium plasma as well as the appearance of plasma instabilities have been discussed and have to be further investigated.

REFERENCES

[1] K. Schulte, "Space Charge Lens for Focusing Heavy Ion Beams", LINAC'10, Tsukuba, Japan, MOP102, (2010).

[2] K. Schulte, "Untersuchung von Messmethoden zur Parameterbestimmung eines Nichtneutralen Plasmas", Diploma Thesis, Goethe-University, Frankfurt a. M., 2008, p. 53-54.

[3] J. Pfister, "Entwicklung und Anwendung schneller Strahldiagnose fuer Ionenstrahlen", PhD Thesis, Goethe-University, Frankfurt a. M., 2010, p. 120-122.

[4] J.B. Boffard, "Application of excitation cross sections to optical plasma diagnostics", J. Phys. D: Appl. Phys. 37 (2004), R150-R151.

[5] A. R. Filipelli et al., "Principles and Methods for Measurement of Electron Impact Excitation Cross Sections for Atoms and Molecules by Optical Techniques", Advances in Atomic, Molecular, and Optical Physics, Vol. 33 (1994), p. 3-10.

[6] J. H. Lees, "The Excitation Function of Helium", H. H. Wills Physical Laboratory, University of Bristol, 1932, p. 173-186.

[7] W. Knauer, "Diocotron Instability in Plasmas and Gas Discharges", J. Appl. Phys. 37 (1966), p. 602.

[8] M. Droba, "Entwicklung eines numerischen Modells zur Untersuchung von Instabilitaeten in toroidal eingeschlossenen nichtneutralen Plasmen", private communication, 2005.